

Cluster growth of Al on stepped and unstepped GaAs(110) at 300 K: A scanning-tunneling-microscopy examination

J. C. Patrin, Y. Z. Li, and J. H. Weaver

Department of Materials Science and Chemical Engineering, University of Minnesota, Minneapolis, Minnesota 55455

(Received 20 May 1991; revised manuscript received 29 August 1991)

Aluminum nucleation and growth on GaAs(110) was studied with scanning tunneling microscopy (STM). The STM images for growth at 300 K demonstrate three-dimensional cluster formation on atomically flat surfaces, even for 0.015-monolayer (ML) deposition. Clusters with diameters ranging from 35 to 60 Å were produced by the deposition of ~ 0.3 ML of Al. Deposition onto GaAs(110) surfaces with single-height $[1\bar{1}0]$ steps also resulted in cluster formation, with no evidence of preferred decoration of step edges. Displacement of small clusters by the tip revealed undisrupted GaAs(110) surface regions, but tip interactions with large clusters left cluster remnants. The differences suggest Al-GaAs intermixing for the larger clusters.

INTRODUCTION

The processes associated with metal-semiconductor interface formation have been studied for many years.¹ One of the many interfaces investigated, Al/GaAs(110), has received considerable theoretical²⁻⁶ and experimental⁷⁻¹⁴ attention. Zunger³ predicted that Al deposition would yield three-dimensional clusters rather than an ordered overlayer characterized by distinct bonding sites coordinated to As or Ga. Ihm and Joannopoulos⁴ calculated the Al chemisorption energy for a single atom per unit cell and then determined the adsorption energy contour on GaAs(110). Energy minimization for two atoms per unit cell suggested that Al clusters would be more stable than chains of chemisorbed atoms. They also predicted that activation energies for Al diffusion along the $[1\bar{1}0]$ direction would be 0.5 eV for motion between the zigzag chains and ~ 0.3 eV atop the zigzag chains, concluding that diffusion at 300 K was likely. Zhang, Cohen, and Louie⁵ used *ab initio* pseudopotential calculations for thick Al overlayers and predicted that the GaAs(110) surface would unrelax as the interface was formed. They also concluded that metal-induced gap states were not sensitive to the interface geometry and that the local density of states was sufficient to pin the Fermi level. Klepeis and Harrison⁶ used the tight-binding formalism to determine bonding sites for individual atoms on GaAs(110), finding that the lowest energy site for Al involved bonding to a Ga atom.

Experimentally, interface formation for Al/GaAs(110) has been investigated for growth temperatures from 60 to 300 K. Photoemission spectroscopy,^{7,8,10-12} Auger spectroscopy,^{9,11} low-electron energy diffraction,⁹ electron-energy-loss spectroscopy,¹³ and medium-energy ion-scattering¹⁴ studies have shown Al cluster formation but also Al-GaAs reaction during growth at 300 K. Deposition onto substrates at low temperature produced a more planar Al overlayer because of suppressed diffusion,⁹⁻¹³ but interfacial reaction was not quenched.¹² Chang *et al.*¹⁵ studied the influence of steps and step orienta-

tions in growth kinetics of Al on GaAs(100) and concluded that steps were active sites where Al nucleation was favored. Still unresolved, however, was the issue of how reaction was initiated on the surface, given the weak interaction of individual Al atoms with the surface and the strong evidence for intermixing.

This paper focuses on the growth of three-dimensional Al clusters on flat and stepped GaAs(110). The goal was to determine the microscopic profile of the surface with the hope that distinguishing characteristics would be found that would reflect the transition from clusters to reaction products. The measurements show small Al clusters having diameters of ~ 20 Å (~ 40 atoms) for Al depositions of $\Theta=0.015$ ML at 300 K. For $\Theta=0.3$ ML, the surface was decorated with clusters having diameters ranging from ~ 35 to ~ 60 Å. We found no evidence that clustering occurred preferentially at $[1\bar{1}0]$ steps. Cluster displacements by the tip made it possible to observe portions of the substrate previously covered by the cluster. When the clusters were small, examination of the exposed regions with atomic resolution showed that the underlying areas were not disrupted. When the clusters were large, however, tip interactions left remnants of the clusters. We attribute the difference to the onset of reaction triggered by the instability of the growing clusters on the surface, i.e., Al-GaAs intermixing occurred at the boundary between the large clusters and the substrate. Although the atomic content of the remnant clusters could not be determined with STM, we are guided in our interpretation by previous studies of Al-GaAs interface formation and chemical mixing. We note that cluster growth and overlayer instabilities have been observed previously with STM for Cr/GaAs(110) (Ref. 16) and Sm/GaAs(110) (Ref. 17).

EXPERIMENT

The STM experiments were performed in an ultrahigh vacuum chamber at a pressure of $\sim 6 \times 10^{-11}$ Torr using a commercial microscope.¹⁸ GaAs(110) surfaces were

prepared by cleaving $2 \times 3 \times 10 \text{ mm}^3$ posts doped with Si at $4 \times 10^{18} \text{ cm}^{-3}$. Tungsten tips were prepared by electrochemical etching in 10 wt% KOH in H_2O . Before use, they were cleaned *in situ* by electron bombardment heating. Aluminum was evaporated from resistively heated W baskets. The deposition rate was 0.5–2 Å/min, and the pressure during evaporation was lower than 4×10^{-10} Torr. Aluminum coverages were determined by a quartz-crystal microbalance. One monolayer (ML) on the GaAs(110) surface corresponds to 1.47 Å of Al, assuming two atoms per surface-unit cell with a surface atomic density of $8.85 \times 10^{14} \text{ atoms cm}^{-2}$. The STM images were taken in the constant-current mode with currents between 0.1 and 1 nA. The tip was biased positive relative to the sample with voltages ranging from 2 to 4 V. The images shown here were not corrected for thermal drift.

RESULTS AND DISCUSSION

The cleaved GaAs(110) surface has been well characterized with STM images obtained using positive- and

negative-tip biases to emphasize As and Ga sites, respectively.¹⁹ Although most studies have focused on the ideal surface, Yang *et al.*²⁰ recently examined steps on GaAs(110) created by cleaving. During the course of these studies, we have been able to examine Al deposition with both ideal and stepped surfaces where the steps were single-height $[1\bar{1}0]$ steps. Al deposition onto such surfaces allowed an assessment of their effect on clustering. The terrace width ranged from ~ 50 –1000 Å over the region explored.

Figure 1(a) shows a mosaic of images for 0.015 ML of Al condensed at 300 K onto a stepped GaAs(110) surface. The rows of As atoms are clearly visible along the $[1\bar{1}0]$ direction of the large terraces. Roughly parallel steps run from upper left to lower right along $[1\bar{1}0]$. The large terrace on the left half of the mosaic is also terminated by an irregular step (*I*) in the center of the figure. The bright features at the irregular step edge are small Al clusters. The number density of small clusters along these steps appears to be higher than along $[1\bar{1}0]$ steps. Such irregular steps are relatively rare, but we speculate that the

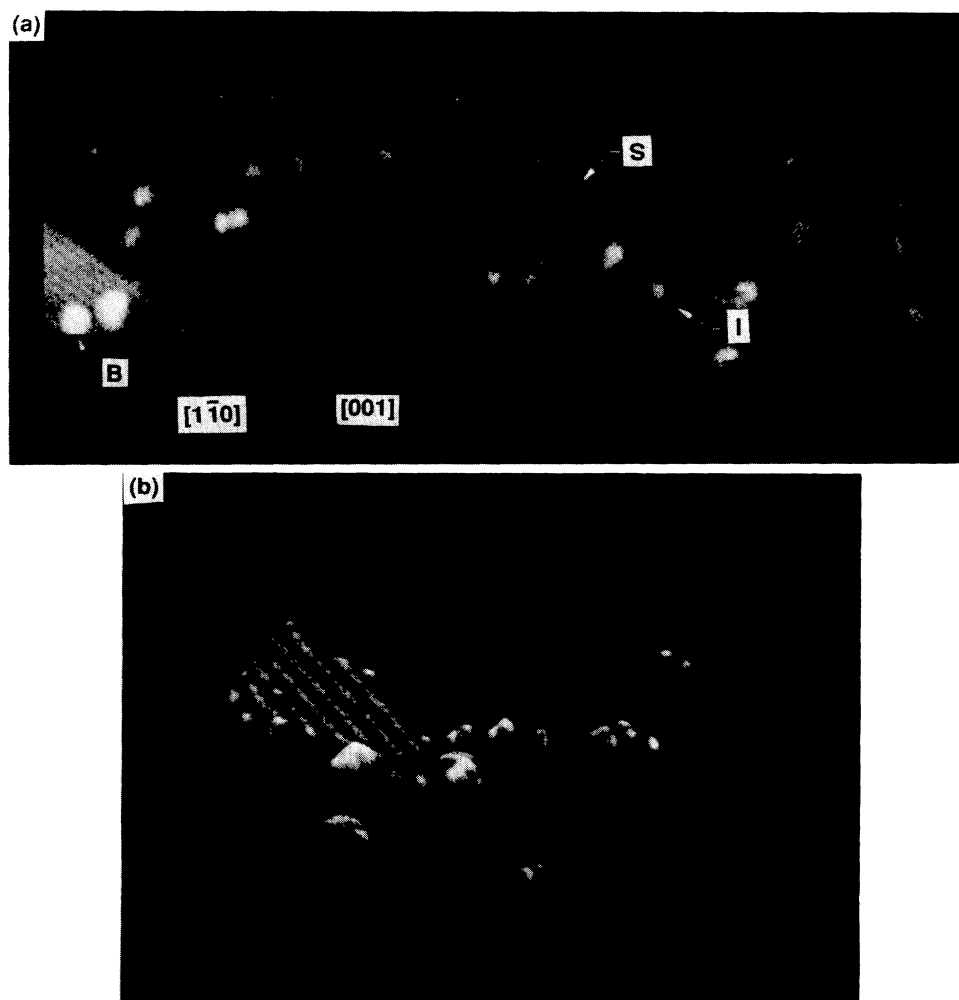


FIG. 1. STM images and a cross section for 0.015-ML Al deposition on a stepped GaAs(110) interface at 300 K. (a) $475 \times 125 \text{ \AA}^2$ area acquired with a tip bias of 3.8 V and 0.1 nA showing large terraces decorated with Al clusters, $[1\bar{1}0]$ steps (labeled *S*) with almost no Al, and clusters at the irregular terminals of the large terrace (labeled *I*). (b) A $125 \times 125 \text{ \AA}^2$ 3D rendered image displayed to enhance the curvature.

higher cluster density results because Al diffusion is perpendicular to these steps. In addition, the accommodation coefficient at these steps may be higher than that for $[1\bar{1}0]$ steps because of the increased number of dangling bonds. Significantly, the results of Fig. 1 for a stepped surface show that the more regular $[1\bar{1}0]$ steps do not serve as preferred nucleation sites for Al. The deposition of 0.015 ML of Al produced clusters on the terraces that contain as many as ~ 40 atoms. The volume of the cluster labeled *B* at the left of Fig. 1(a) was estimated to be 535 \AA^3 , corresponding to ~ 32 atoms, as determined by integrating the height contours of the STM image.^{21,22} A 3D-rendered image from the mosaic of Fig. 1(a) that enhances the curvature is shown in Fig. 1(b) to provide a better perspective of cluster heights relative to the contact area. It was not possible to determine a favored chemisorption site at 300 K because cluster formation occurred even for the lowest coverage studied (0.015 ML). Clustering of Al adatoms is not surprising because of the active diffusion of individual adatoms. The hopping frequency of an adatom having sufficiently thermal energy to surmount the potential barrier E_b for surface diffusion can be approximated by $\nu_d \exp(-E_b/kT)$, where ν_d is the substrate vibrational frequency. Such thermally activated hopping is very probable based on estimates using typical vibrational frequencies and the barrier for diffusion calculated by Ihm and Joannopoulos.⁴

The STM results provide particularly important insight into the bonding of the clusters to the surface because clusters were occasionally displaced by the tip. This occurred for $< 5\%$ of the images. Figure 2(a) shows a STM image of a highly stepped surface onto which 0.07 ML of Al had been deposited. The arrow indicates a cluster with a diameter of 25 \AA and a height of $\sim 5 \text{ \AA}$ consisting of ~ 40 atoms situated on a step. This cluster

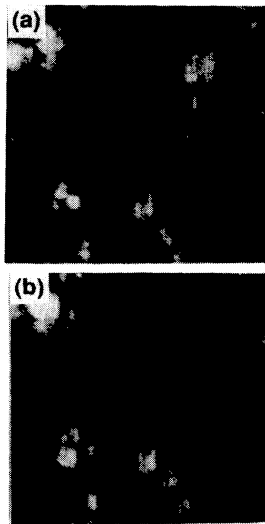


FIG. 2. STM images for 0.07 ML of Al on a stepped GaAs(110) surface. Both images are $100 \times 100 \text{ \AA}^2$ and were obtained with a tip bias of 2.5 V and a tunneling current of 0.6 nA. The cluster bonded to the step (a) was displaced after repeated scanning and the now-exposed area (b) shows no modification of the surface beneath the small cluster.

was displaced upon subsequent scanning, as shown by Fig. 2(b). The other surface features appeared unchanged, and the atomic resolution of the tip was maintained. Examination of Fig. 2(b) shows that the substrate exposed by cluster displacement was not disordered or in any way different from other equivalent sites on the surface. We conclude that the cluster with ~ 40 atoms was weakly interacting with the substrate and had not induced surface disruption. This is particularly intriguing because the heat of formation for AlAs is 10 kcal/mole higher than that for GaAs, and intermixing at the interface has been reported at higher coverage (but not < 0.1 ML). As will be discussed for higher coverages, however, remnants of larger clusters were left behind on the surface.

Tip-cluster interactions sufficient to move two-dimensional islands have been observed for Ag/Si(100).^{23,24} In that case, the Si substrate beneath the two-dimensional island remained ideal. For Ag deposition on GaAs(110), Trafas *et al.*²⁵ observed that a Ag cluster containing ~ 100 atoms was displaced and attached with a larger cluster. Again, the exposed substrate remained undisrupted. These observations were easily reconciled by noting that interactions of the cluster with the substrate was weak and Ag—Ag bonding was strong.

Figure 3(a) shows a $1400 \times 1400 \text{ \AA}^2$ image obtained after 0.3-ML deposition of Al on a surface with $[1\bar{1}0]$ monatomic steps defining large terraces. In addition, there is a pointed peninsulalike structure that originates at the upper left and terminates near the lower right. It is one layer higher than the terrace beneath it. In this case, the Al clusters were typically $35\text{--}60 \text{ \AA}$ in diameter and $8\text{--}15 \text{ \AA}$ high. Figure 3(b) shows a higher resolution image of the part in Fig. 3(a) defined by the box. The volume of the typical cluster labeled *A* was $\sim 4760 \text{ \AA}^3$ and the contact area was $\sim 1520 \text{ \AA}^2$, corresponding to a cluster containing ~ 290 atoms. In addition, there are small protrusions along the $[1\bar{1}0]$ steps that have been observed on clean cleaved stepped surfaces; they are not due to Al accumulation at the steps. Figure 3(c) is a $400 \times 400 \text{ \AA}^2$ step-free area that demonstrates that similar cluster size distributions are obtained for $[1\bar{1}0]$ -stepped and -unstepped surfaces.

Examination of Figs. 3(a) and 3(c) indicates that the clusters were randomly distributed on stepped and unstepped surfaces, with no indication of preferential bonding at $[1\bar{1}0]$ steps. Indeed, the density was $1\text{--}3 \times 10^{12}$ clusters/cm² on both $[1\bar{1}0]$ -stepped and -unstepped surfaces for 0.3-ML deposition with cluster diameters ranging from 35 to 60 \AA . In contrast, Chang *et al.*¹⁵ deposited 5 \AA of Al on miscut GaAs(100) containing $[110]$ and $[111]$ steps and concluded from photoemission measurements that those stepped surfaces had increased surface reaction compared to flat (100) surfaces. They associated the increased reactivity with the larger number of dangling bonds. It will be intriguing to examine the different morphologies of these surfaces with STM to see how Al deposition on miscut GaAs(100) produces enhanced nucleation.

Comparison of Figs. 3(a) and 3(b) reveals that the 50-

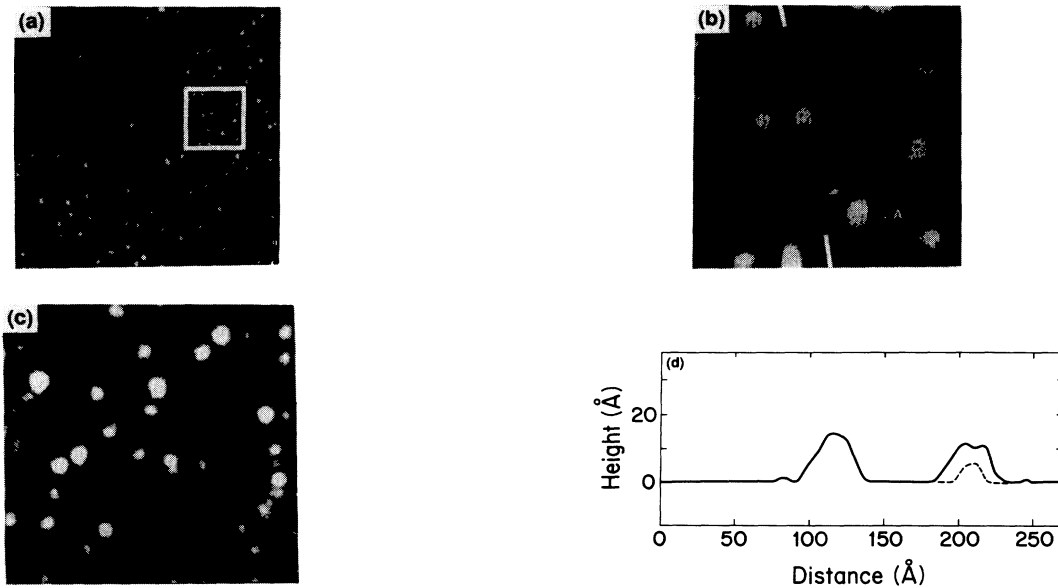


FIG. 3. STM images showing a GaAs(110) surface with $[1\bar{1}0]$ steps onto which 0.3 ML of Al has been deposited. The clusters appear randomly distributed with no preferential bonding to the step edges. (a) A $1400 \times 1400 \text{ \AA}^2$ image acquired with a tip bias of 3 V and 0.1 nA. (b) A higher resolution $260 \times 260 \text{ \AA}^2$ image of the boxed region in (a). The cluster marked by an arrow in (a) is missing in (b); the remnant cluster is marked with an arrow. (c) A $400 \times 400 \text{ \AA}^2$ image of clusters on a step-free area. (d) A cross section of the cluster identified in (a) and (b) before (solid line) and after removal (dashed line).

\AA -diam cluster marked by an arrow in Fig. 3(a) was partially removed upon subsequent scanning. The remnant cluster was $\sim 25 \text{ \AA}$ in diameter and 5 \AA in height, as shown by the cross sections in Fig. 3(d) measured before and after removal. For Al on GaAs(110), the largest cluster that did not leave behind a footprint was 25 \AA in diameter (~ 40 atoms); clusters that left behind remnants were $35\text{--}50 \text{ \AA}$ in diameter ($\sim 115\text{--}300$ atoms). The complete displacement of smaller clusters was observed 20 times during our measurements and the partial removal of larger clusters occurred five times. We associate the remnant cluster with Al-GaAs intermixing beneath the cluster, even though the atomic makeup of the remnant could not be determined with STM. As an alternate explanation, it could be argued that the force exerted by the tip was incapable of completely removing larger clusters because they were larger and had greater surface contact. However, once the fragmentation was created, it remained at the same place, with no subsequent tip effects observed during repeated scans. As for the case of small and large clusters, the remnant cluster did not show any order. Attributing the remnant cluster to atomic intermixing beneath a large cluster is in agreement with medium-energy ion-scattering¹⁴ results where chemical reactions beneath the clusters were reported. In addition, photoemission results for Al coverages as low as 0.14 ML have demonstrated that Ga atoms released from the substrate mix and segregate on the clusters.¹² Indeed, the issue has not been whether the Al-GaAs interface exhibits reaction but rather why Al is so mobile that clusters, which represent the precursors to reaction, form on the surface.

Zunger³ has suggested that reaction beneath large clusters may occur because the condensation energy released upon clustering is sufficient to promote local chemical re-

actions. Although the dynamics of the process is not known, the cluster size plays an important role in determining whether the cluster is stable or not on GaAs(110). A critical coverage threshold has also been used to explain photoemission results for Ce growth on Si(111) when a cluster-induced reaction was observed for Ce coverages $\geq 0.6 \text{ ML}$.²⁶ Trafas *et al.*¹⁶ showed that Cr clusters formed at low coverage but also that those with diameters as small as 20 \AA had induced intermixing with the surface and had incorporated Ga and As atoms.

Insight into the growth of Al clusters was obtained by comparing volumes to areas in contact with the substrate. The volumes were determined by integrating height contours from the STM images, as has been done elsewhere.^{21,22} Cluster volumes were measured for five Al coverages from 0.07 to 0.8 ML and with different tips to ensure reproducibility. A two-parameter fit was used for the power-law equation $V = CA^n$, where V is the volume and A is the contact area. Figure 4 shows the data for more than 70 clusters together with the best fit obtained for $n = 1.19$. For comparison, Fig. 4 also shows the behavior expected for hemispherical growth of $V = (2/3\sqrt{\pi})A^{1.5}$ and for 2D growth $V = 1.47A$. Here 1.47 is the thickness of one Al monolayer in angstroms on the GaAs(110) surface. We find that the clusters are more two dimensional in shape for Al deposition at 300 K. It is interesting to compare these results to those for Fe/GaAs(110) where the best fit to the power law for growth at 300 K was with $n = 1.2$. For Fe/GaAs(110) where Fe deposition promotes the release of Ga and As atoms, those released atoms become incorporated in the clusters and their presence may affect cluster growth. Unfortunately, STM is unable to distinguish atomic species in the clusters, identifying the segregated Ga and

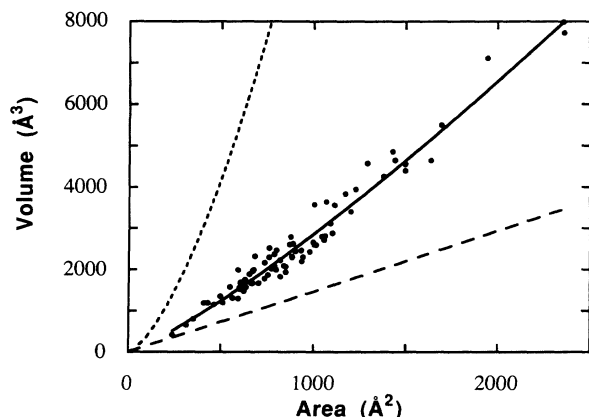


FIG. 4. Cluster volume vs area for various Al coverages. The solid line is the best fit to the cluster volume area power law with $V = CA^{1.19}$. The short-dashed line depicts ideal hemispherical growth, $V = (2/3\sqrt{\pi})A^{1.5}$, and the long-dashed line is for 2D growth, $V = 1.47A$.

As atoms observed with photoemission. For the nonreactive Ag/GaAs(110) system,²⁵ the best fit gave $n = 1.57$.

Figure 5 shows an STM image for 30 Å of Al deposited on a stepped GaAs(110) surface. The image and cross sections of various features of the surface demonstrate that the surface roughness does not change appreciably with growth. Indeed, the grain size of the polycrystalline film observed after 100-Å deposition resembled those at 10 and 30 Å, and there was no tendency to form an atomically smooth surface (surface rms roughness 2.5–3.5 Å). The maximum peak-to-valley distance was ~ 25 Å for the 30-Å coverage and the height-to-diameter aspect ratio of a typical grain was ~ 0.25 . In Fig. 5, the grains appear to be aligned along the substrate $[1\bar{1}0]$ direction but other images show different alignment. We speculate that the fine-grain structure results from the small ratio of the substrate temperature during deposition to the melting temperature of Al. Increasing the substrate temperature will probably result in larger grains because of the increased Al surface diffusion.

There is no evidence of the formation of clusters evolving into distinct crystallites with faceted surfaces for Ag/GaAs(110) growth at 300 K. Instead, the fine-grained morphology resembles that for the weakly reac-



FIG. 5. STM image of 30 Å of Al on GaAs(110). This $1400 \times 1400 \text{ Å}^2$ image was obtained with a tip bias of 3.1 V and tunneling current of 0.15 nA. It shows surface grains with sizes up to 60 Å and an overall rms surface roughness of 2.5–3.5 Å. The alignment probably reflects the existence of multiple height steps on the cleaved surface. Growth to 100 Å of Al at 300 K resulted in equivalent surface roughness and appearance.

tive Fe/GaAs(110) interface where Dragoset *et al.*²² reported features with 40–50 Å diameters and a rms roughness of ~ 3 Å after 10-Å deposition of Fe. The evolution of the reactive Cr/GaAs(110) interface¹⁶ showed similar asperities for all coverages and a surface rms roughness of ~ 2.3 Å after 5-ML deposition. In each case, growth is influenced by kinetic constraints but we suggest that it is also influenced by the presence of Ga and/or As atoms in the surface region. These atoms are released during the early stages of overlayer formation (Cr, Fe, Al but not Ag) but are not trapped at the buried interface.²⁷ Instead, they continue to segregate to the surface region during slow growth at 300 K. For Al/GaAs(110), photoemission results have shown the segregation of Ga because of its low solubility in the growing Al layer. These atoms should have an effect on the growth structures and the kinetics, but the details in terms of local bonding configurations and surface-free energies are not yet known. In any case, disruption occurs despite the fact that the lattice mismatch is only $\sim 1.3\%$.⁵

ACKNOWLEDGMENTS

This work was supported by the Office of Naval Research. Cheerful support from Park Scientific Instruments is gratefully acknowledged.

¹See, for example, J. H. Weaver, in *A New Era of Materials Science*, edited by J. R. Chelikowsky and A. Franciosi (Springer-Verlag, Berlin, 1991), Chap. 8 and references therein.

²C. A. Swarts, J. J. Barton, W. A. Goddard, and T. C. McGill, *J. Vac. Sci. Technol.* **17**, 869 (1980).

³A. Zunger, *Phys. Rev. B* **24**, 4372 (1981); *J. Vac. Sci. Technol.* **19**, 690 (1981).

⁴J. Ihm and J. D. Joannopoulos, *Phys. Rev. B* **26**, 4429 (1982).

⁵S. B. Zhang, M. L. Cohen, and S. G. Louie, *Phys. Rev. B* **34**, 768 (1986).

⁶J. E. Klepeis and W. A. Harrison, *Phys. Rev. B* **40**, 5810 (1989).

⁷R. R. Daniels, A. D. Katnani, T-X. Zhao, G. Margaritondo, and A. Zunger, *Phys. Rev. Lett.* **49**, 895 (1982).

⁸N. G. Stoffel, M. K. Kelly, and G. Margaritondo, *Phys. Rev. B* **27**, 6561 (1983).

⁹C. R. Bonapace, K. Li, and A. Kahn, *J. Phys. (Paris) Colloq.* **45**, 409 (1984).

¹⁰K. Stiles, A. Kahn, D. G. Kilday, and G. Margaritondo, *J. Vac. Sci. Technol. B* **5**, 987 (1987).

¹¹R. Cao, K. Miyano, T. Kendelewicz, K. K. Chin, I. Lindau, and W. E. Spicer, *J. Vac. Sci. Technol. B* **5**, 998 (1987).

- ¹²S. G. Anderson, C. M. Aldao, G. D. Waddill, I. M. Vitomirov, S. J. Severtson, and J. H. Weaver, *Phys. Rev. B* **40**, 8305 (1989), and references therein.
- ¹³C. R. Bonapace, D. W. Tu, and A. Kahn, *J. Vac. Sci. Technol. B* **3**, 1099 (1985).
- ¹⁴L. Smit and J. F. van der Veen, *Appl. Surf. Sci.* **26**, 230 (1986).
- ¹⁵S. Chang, L. J. Brillson, Y. J. Kime, D. S. Rioux, P. D. Kirchner, G. D. Petit, and J. M. Woodall, *Phys. Rev. Lett.* **64**, 2551 (1990).
- ¹⁶B. M. Trafas, D. M. Hill, P. J. Benning, G. D. Waddill, Y.-N. Yang, R. L. Siefert, and J. H. Weaver, *Phys. Rev. B* **43**, 7174 (1991).
- ¹⁷B. M. Trafas, D. M. Hill, R. L. Siefert, and J. H. Weaver, *Phys. Rev. B* **42**, 3231 (1990).
- ¹⁸Sang-il Park and C. F. Quate, *Rev. Sci. Instrum.* **58**, 2010 (1987); Park Scientific Instruments, Mountain View, CA 94043.
- ¹⁹R. M. Feenstra, J. A. Stroscio, J. Tersoff, and A. P. Fein, *Phys. Rev. Lett.* **58**, 1192 (1987).
- ²⁰Y.-N. Yang, B. M. Trafas, R. L. Siefert, and J. H. Weaver, *Phys. Rev. B* **44**, 3218 (1991).
- ²¹P. N. First, J. A. Stroscio, R. A. Dragoset, D. T. Pierce, and R. J. Celotta, *Phys. Rev. Lett.* **63**, 1416 (1989).
- ²²R. A. Dragoset, P. N. First, J. A. Stroscio, D. T. Pierce, and R. J. Celotta, *Mat. Res. Soc. Symp. Proc.* **151**, 193 (1989).
- ²³T. Hashizume, R. J. Hamers, J. E. Demuth, K. Markert, and T. Sakurai, *J. Vac. Sci. Technol. A* **8**, 249 (1990).
- ²⁴A. Brodde, D. Badt, S. Tosch, and H. Neddermeyer, *J. Vac. Sci. Technol. A* **8**, 251 (1990).
- ²⁵B. M. Trafas, Y.-N. Yang, R. L. Siefert, and J. H. Weaver, *Phys. Rev. B* **43**, 14107 (1991).
- ²⁶M. Grioni, J. Joyce, S. A. Chambers, D. G. O'Neill, M. del Giudice, and J. H. Weaver, *Phys. Rev. Lett.* **53**, 2331 (1984).
- ²⁷J. H. Weaver, Z. Lin, and F. Xu, in *Surface Segregation Phenomena*, edited by P. A. Dowben and A. Miller (CRC, Boca Raton, FL, 1990), Chap. 10, pp. 369–457.

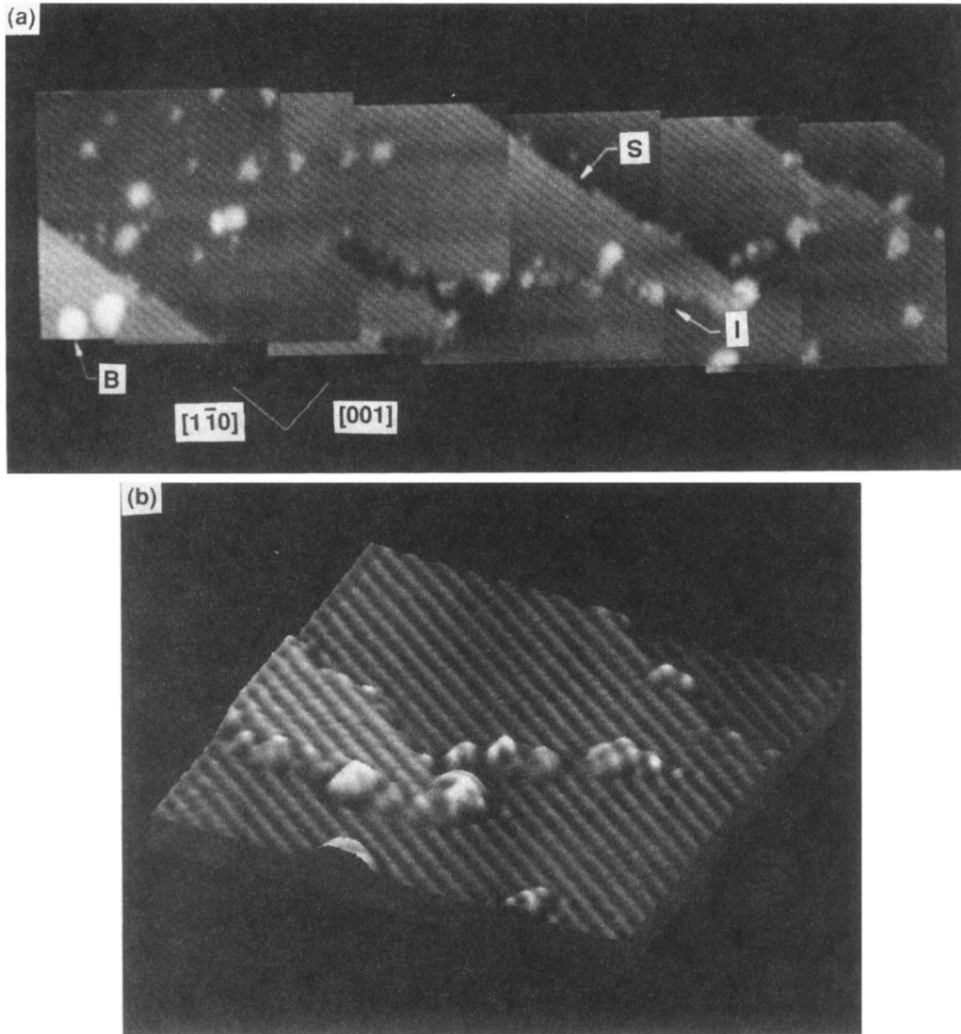


FIG. 1. STM images and a cross section for 0.015-ML Al deposition on a stepped GaAs(110) interface at 300 K. (a) $475 \times 125 \text{ \AA}^2$ area acquired with a tip bias of 3.8 V and 0.1 nA showing large terraces decorated with Al clusters, $[1\bar{1}0]$ steps (labeled *S*) with almost no Al, and clusters at the irregular terminals of the large terrace (labeled *I*). (b) A $125 \times 125 \text{ \AA}^2$ 3D rendered image displayed to enhance the curvature.

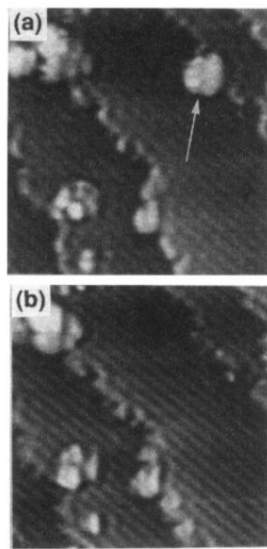


FIG. 2. STM images for 0.07 ML of Al on a stepped GaAs(110) surface. Both images are $100 \times 100 \text{ \AA}^2$ and were obtained with a tip bias of 2.5 V and a tunneling current of 0.6 nA. The cluster bonded to the step (a) was displaced after repeated scanning and the now-exposed area (b) shows no modification of the surface beneath the small cluster.

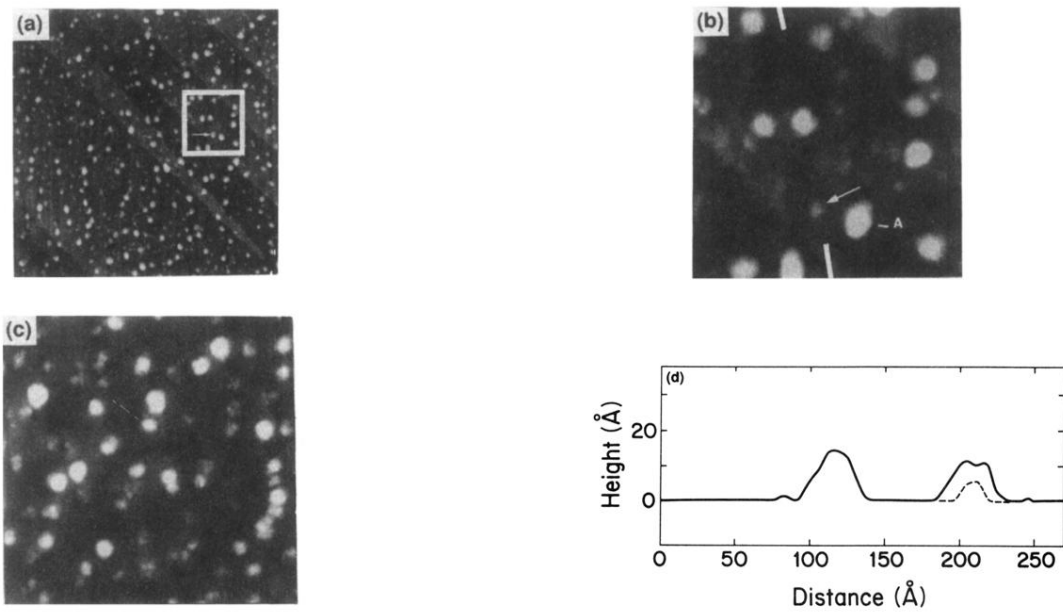


FIG. 3. STM images showing a GaAs(110) surface with $[1\bar{1}0]$ steps onto which 0.3 ML of Al has been deposited. The clusters appear randomly distributed with no preferential bonding to the step edges. (a) A $1400 \times 1400 \text{ \AA}^2$ image acquired with a tip bias of 3 V and 0.1 nA. (b) A higher resolution $260 \times 260 \text{ \AA}^2$ image of the boxed region in (a). The cluster marked by an arrow in (a) is missing in (b); the remnant cluster is marked with an arrow. (c) A $400 \times 400 \text{ \AA}^2$ image of clusters on a step-free area. (d) A cross section of the cluster identified in (a) and (b) before (solid line) and after removal (dashed line).

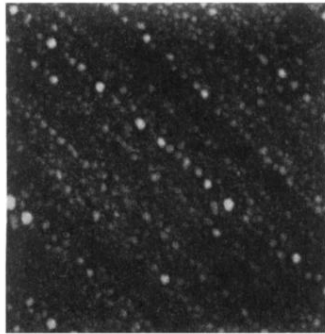


FIG. 5. STM image of 30 Å of Al on GaAs(110). This $1400 \times 1400 \text{ \AA}^2$ image was obtained with a tip bias of 3.1 V and tunneling current of 0.15 nA. It shows surface grains with sizes up to 60 Å and an overall rms surface roughness of 2.5–3.5 Å. The alignment probably reflects the existence of multiple height steps on the cleaved surface. Growth to 100 Å of Al at 300 K resulted in equivalent surface roughness and appearance.